

Focusing microparticles in a microfluidic channel with standing surface acoustic waves (SSAW)[†]

Jinjie Shi,^a Xiaole Mao,^{ab} Daniel Ahmed,^a Ashley Colletti^{‡a} and Tony Jun Huang^{*ab}

Received 23rd October 2007, Accepted 6th December 2007

First published as an Advance Article on the web 20th December 2007

DOI: 10.1039/b716321e

We introduce a novel on-chip microparticle focusing technique using standing surface acoustic waves (SSAW). Our method is simple, fast, dilution-free, and applicable to virtually any type of microparticle.

The integration of microfluidics with single microparticle detection techniques enables the development of miniaturized platforms for flow cytometry¹ and fluorescence activated cell sorting (FACS).² In these applications, fluorescently labelled microparticles (*i.e.*, cells) are excited by a laser that is focused on a small volume within a microchannel to allow for accurate detection and sorting. However, because the dimensions of a laser's focal volume are often smaller than those of a microchannel, many species of interest pass by the focal volume without being excited or detected. Therefore, a microparticle focusing technique is often required to constrain the distribution of the microparticles so that all the particles can be registered by the detector. It also facilitates particle sorting by lining up the particles in the microfluidic channel.

To date, many microparticle-focusing techniques have been developed, including hydrodynamic focusing,^{3,4} electro-kinetic focusing,⁵ and dielectrophoresis (DEP) focusing.⁶ In hydrodynamic focusing, the microparticle suspension is constrained in the middle of the channel by outer sheath flows of higher flow rates. The introduction of excessive sheath solution, however, dilutes and disperses the sample. Other techniques, such as electro-kinetic focusing or DEP focusing, focus the microparticles by creating a force field applied directly to microparticles themselves. These methods do not require an additional sheath solution, but they are only applicable to certain types of microparticles: electro-kinetic focusing is only for charged species, and DEP focusing relies on the polarizability of the particles.

Acoustic waves generate pressure gradients in a liquid that can be used to manipulate suspended particles⁷ or liquid medium.⁸ Such acoustic-based methods are ideal for on-chip microparticle focusing, since they do not need a sheath solution and can be used to focus virtually any microparticle. Recent developments in

acoustophoresis have enabled the separation of microparticles of different sizes and densities in microfluidic channels by using standing bulk acoustic waves (BAW).^{9,10} The standing waves were formed by coupling the acoustic waves from the substrate-bonded bulk transducer within the microchannel, which acted as a resonance cavity.^{9,10} This mechanism can potentially be used to focus particles or biomolecules in microfluidic channels. However, the formation of standing BAW in these single-transducer resonating systems requires that the channel material possess excellent acoustic reflection properties. Soft polymer materials such as polydimethylsiloxane (PDMS) that are commonly used in microfluidic applications have poor reflection properties. Therefore, the requirement of high acoustic reflection makes it challenging to implement these single-transducer BAW-based techniques with fast prototyping methods, such as soft lithography, that are widely used in microfluidics. While dual-transducer non-resonating BAW-based systems are compatible with soft lithography techniques,^{11,12} the complex designs of these systems make them less attractive.

In this work we introduce a novel standing surface acoustic wave (SSAW) focusing technique that uses a PDMS channel fabricated by standard soft lithography. A schematic of the SSAW focusing device is shown in Fig. 1. A pair of interdigital transducers (IDTs) are deposited on a piezoelectric substrate, and

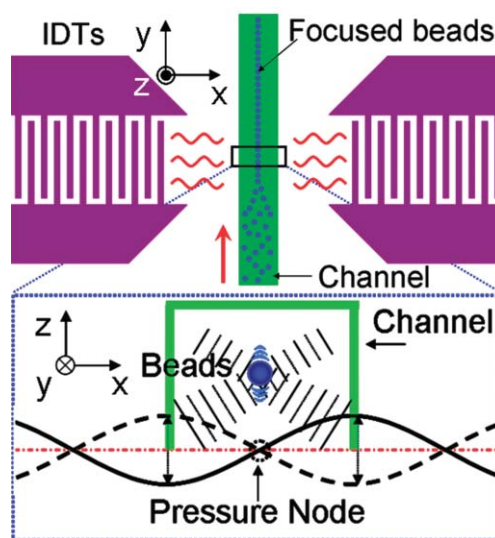


Fig. 1 Schematic of the SSAW focusing device, illustrating its working mechanism. The channel width is designed to cover only one pressure node such that beads are focused at that node when the SSAW is generated. Inset: illustration of the SSAW pressure field inside the channel, where the beads are focused at the pressure node.

^aDepartment of Engineering Science and Mechanics, The Pennsylvania State University, University Park, PA, 16802, USA.
E-mail: junhuang@psu.edu; Fax: +1 814-865-9974;
Tel: +1 814-863-4209

^bDepartment of Bioengineering, The Pennsylvania State University, University Park, PA, 16802, USA

[†] Electronic supplementary information (ESI) available: Fabrication process of the device (Fig. S1); PDMS microchannel and SAW substrate alignment (Fig. S2); real-time video of fluorescent polystyrene beads focusing inside a microchannel. See DOI: 10.1039/b716321e

[‡] NNIN summer REU student. Present address: Department of Biomedical Engineering, Johns Hopkins University, Baltimore, MD 21218, USA.

a PDMS-based microfluidic channel is bonded with the substrate and positioned between the two IDTs. Microparticle solutions are infused into the microfluidic channel by a pressure-driven flow. Once an RF signal is applied to both IDTs, two series of surface acoustic waves (SAW) propagate in opposite directions toward the particle suspension solution inside the microchannel. The constructive interference of the two SAW result in the formation of a SSAW, as well as the periodic distribution of the pressure nodes (minimum pressure amplitude) and anti-nodes (maximum pressure amplitude) on the substrate. When the SSAW encounter the liquid medium inside the channel, leakage waves in the longitudinal mode are generated, causing pressure fluctuations in the medium.¹⁰ These pressure fluctuations result in acoustic radiation forces that act laterally (in the x -direction of Fig. 1) on the particles.^{10,13–15} As a result, the suspended particles inside the channel will be forced toward either the pressure nodes or antinodes, depending on the density and compressibility of the particles and the medium. When the channel width covers only one pressure node (or antinode), the particles will be trapped in that node and consequently, focusing is achieved.

Fig. 2 shows the device used in our study. A $Y + 128^\circ X$ -propagation lithium niobate (LiNbO_3) piezoelectric wafer (500 μm thick) was used as the substrate due to its high coupling coefficient in SAW generation. The two IDTs were arranged parallel to each other, and were formed by e-beam evaporation of Ti (50 \AA , adhesive layer) and Au (800 \AA). The period of the IDTs was 100 μm and each IDT electrode was 9 mm long and 25 μm wide. A PDMS microchannel with a width and depth of 50 μm and a length of 1.3 cm was bonded to the LiNbO_3 substrate and aligned between the two IDTs. Smooth side openings aligned on either side of the PDMS channel were used to precisely define the working region of the SSAW and reduce the propagation loss.

The bonded device was mounted on the stage of an inverted microscope (Nikon TE2000U). A solution (1.176×10^7 beads ml^{-1}) of fluorescent (Dragon Green) polystyrene particles (diameter 1.9 μm , Bangs Laboratories) was injected into the channel using a syringe pump (KDS210, KD Scientific). An AC signal generated by an RF signal generator (Agilent E4422B) was amplified with a power amplifier (Amplifier Research 100A250A). This signal was split into two coherent signals, which

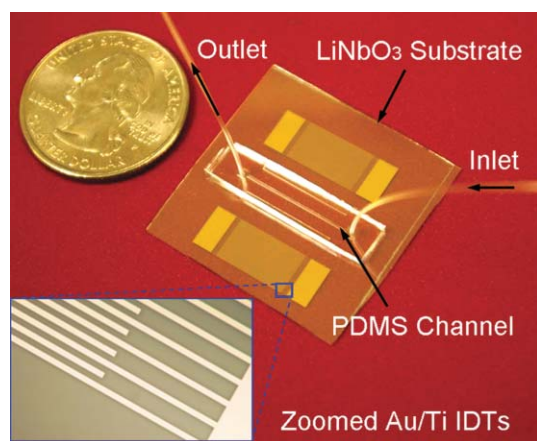


Fig. 2 Photograph of the bonded SSAW focusing device consisting of a LiNbO_3 substrate with two parallel IDTs and a PDMS channel. Inset: zoomed-in photograph of IDTs.

were subsequently applied to the two IDTs to generate SSAW. The signal frequency was set to be 38.2 MHz (resonance frequency) and the applied power was 24 dBm (~ 250 mW).

The distribution of fluorescent microparticles was recorded during the focusing process at four different regions marked as I, II, III and IV in Fig. 3a. Site I was not within the SSAW propagation area, so microparticles barely experienced acoustic forces in this region. As a result, the distribution of microparticles in this region was uniform across the width of the channel (Fig. 3b). As particles entered the area in which the SSAW propagated (Site II), the acoustic force exerted on the particles drove them toward the centre of the channel (where pressure nodes existed), as shown in Fig. 3c. As the particles exited Site II, they were focused into a narrow stream in the middle of the channel. Based on the flow velocity (6.7 cm s^{-1}) and the distance ($\sim 300 \mu\text{m}$) over which the particles travelled from the unfocused site to the totally focused site, we calculated the duration of the focusing process to be 4.5 ms. At Site III, the focused stream was well-stabilized, and the width of the stream was measured to be approximately 5 μm (Fig. 3d)—less than three times the diameter of a single particle, 5% of the SSAW wavelength, and 10% of the channel width. We further monitored the particle distribution at Site IV (Fig. 3e) where SSAW did not propagate, and observed that the width of the focusing stream remained constant. This phenomenon was due to the laminar nature of the flow.¹⁶

We also observed that the SSAW focusing effect was dependent upon the frequency of the acoustic waves. Fig. 4(a) and (b) depict the experimental results monitored from two devices driven at the same power (25 dBm) but different wavelengths ($\lambda_1 = 100 \mu\text{m}$, $\lambda_2 = 200 \mu\text{m}$). The measured focusing width δx_2 ($\sim 10 \mu\text{m}$, Fig. 4b) for Device II was about two times greater than δx_1 ($\sim 5 \mu\text{m}$, Fig. 4a). This observation was due to the balance of acoustic radiation forces and acoustic interparticle forces (*e.g.*, Bjerknes forces, van der Waals force, electrostatic forces), which originated from the acoustic oscillation between particles in the focusing band. When such particles are driven close to each other toward the pressure node by the acoustic radiation forces, the overall

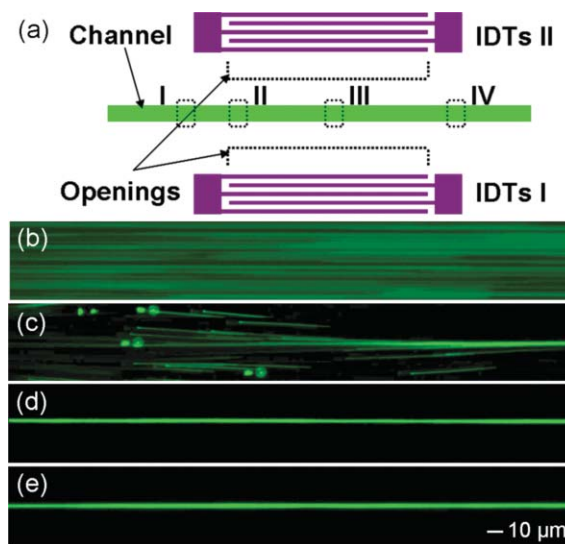


Fig. 3 The schematic in (a) indicates the positions of the chosen sites (I–IV) for monitoring the focusing effect. (b–e) are the recorded fluorescent images at sites (I–IV), respectively.

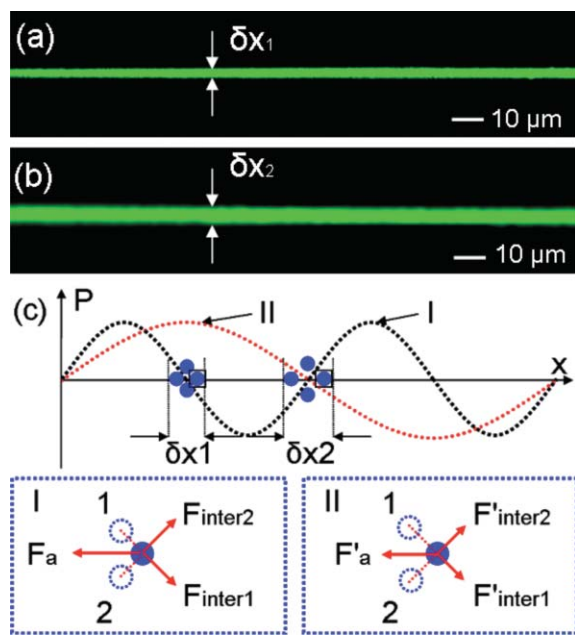


Fig. 4 Experimental data for the focusing performance at a working frequency of (a) 38.2 MHz (corresponding to $\lambda_1 = 100 \mu\text{m}$) and (b) 19.116 MHz (corresponding to $\lambda_2 = 200 \mu\text{m}$). (c) Qualitative analysis of the particle aggregation at pressure nodes at two different working frequencies (drawing not to scale).

effects of the interparticle forces become repulsive to balance the acoustic radiation force.^{13–15} Fig. 4c shows the pressure field and force balance diagram for the particles in Devices I and II; these particles were exposed to acoustic waves with identical pressure amplitude but different wavelengths ($\lambda_2 = 2\lambda_1$). Since the acoustic radiation force exerted on a particle F_a is inversely proportional to its acoustic wavelength, the acoustic radiation force exerted on particles in Device I was twice the force on those in Device II. This higher acoustic radiation force was balanced by a larger repulsive force between particles (Fig. 4c). Therefore, the repulsive force packed the particles closer in Device I (Fig. 4a) than in Device II (Fig. 4b), thereby causing a narrower focusing width in the former device. We expect that sub-micrometer focusing widths can be achieved as we keep increasing the working frequency. This frequency-dependent characteristic presents another advantage of SAW over BAW: it is relatively easy to fabricate IDTs with smaller periods and generate higher-frequency (hundreds of MHz) SAW, while the frequencies for most of the current BAW-based particle manipulating techniques are 1–2 MHz.^{9–12}

In conclusion, we have introduced a novel acoustic manipulation technique, SSAW, to enable fast and effective microparticle

focusing inside a microfluidic channel. In comparison to other particle focusing techniques, including hydrodynamic, electrokinetic and DEP focusing, this method is simple, fast, dilution-free, and can be used to focus virtually any microparticles. Moreover, the transparency of the focusing device makes it compatible with most optical characterization tools used in biology and medicine. In contrast to the BAW-based microparticle manipulation method,^{9–12} the SSAW-based technique localizes most of the acoustic energy on the surface of the substrate and has little loss along the propagation line, thus lowering the power consumption and improving the uniformity of the standing waves. The technique is compatible with standard soft lithography techniques. We expect that it can be used in a wide variety of on-chip biological/biochemical applications.

This research was supported in part by the NSF NIRT grant (ECCS-0609128) and the Penn State Center for Nanoscale Science (MRSEC). Components of this work were conducted at the Penn State node of the NSF-funded National Nanotechnology Infrastructure Network. The authors thank Dr Bernhard R. Tittmann and Subash Jayaraman for help with equipment, and Thomas R. Walker and Michael Lapsley for aid in preparing the manuscript.

Notes and references

- 1 C. Simonnet and A. Groisman, *Anal. Chem.*, 2006, **78**, 5653–5663.
- 2 A. Wolff, I. R. Perch-Nielsen, U. D. Larsen, P. Friis, G. Goranovic, C. R. Poulsen, J. P. Kutter and P. Telleman, *Lab Chip*, 2003, **3**, 22–27.
- 3 P. K. Wong, Y.-K. Lee and C.-M. Ho, *J. Fluid Mech.*, 2003, **497**, 55–65.
- 4 X. Mao, J. R. Waldeisen and T. J. Huang, *Lab Chip*, 2007, **7**, 1260–1262.
- 5 T.-H. Wang, Y. Peng, C. Zhang, P. K. Wong and C.-M. Ho, *J. Am. Chem. Soc.*, 2005, **127**, 5354–5359.
- 6 L. Wang, L. A. Flanagan, N. L. Jeon, E. Monuki and A. P. Lee, *Lab Chip*, 2007, **7**, 1114–1120.
- 7 K. Sritharan, C. J. Strobl, M. F. Schneider, A. Wixforth and Z. Guttenberg, *Appl. Phys. Lett.*, 2006, **88**, 054102.
- 8 H. Yu, J. W. Kwon and E. S. Kim, *Lab Chip*, 2005, **5**, 344–349.
- 9 F. Petersson, L. Aberg, A. M. Sward-Nilsson and T. Laurell, *Anal. Chem.*, 2007, **79**, 5117–5123.
- 10 F. Petersson, A. Nilsson, H. Jönsson and T. Laurell, *Anal. Chem.*, 2005, **77**, 1216–1221.
- 11 M. Wiklund, C. Günther, R. Lemor, M. Jäger, G. Fuhr and H. M. Hertz, *Lab Chip*, 2006, **6**, 1537–1544.
- 12 S. Kapishnikov, V. Kantsler and V. Steinberg, *J. Stat. Mech.*, 2006, 01012.
- 13 T. Uchida, T. Suzuki and S. Shiokawa, in 1995 IEEE Ultrasonics Symposium, held in Seattle, WA, 7–10 Nov 1995, IEEE Press, New York, 1995, vol. 2, pp. 1081–1084.
- 14 L. A. Kuznetsova and W. T. Coakley, *Biosens. Bioelectron.*, 2007, **22**, 1567–1577.
- 15 A. A. Doinikov, *J. Fluid Mech.*, 2001, **444**, 1–21.
- 16 X. Mao, J. R. Waldeisen, B. K. Juluri and T. J. Huang, *Lab Chip*, 2007, **7**, 1303–1308.